

Two-sample comparison through additive tree models for density ratios

Naoki Awaya¹, Yuliang Xu², and Li Ma²

¹*School of Political Science and Economics, Waseda University*

²*Department of Statistics, University of Chicago*

August 19, 2025

Abstract

The ratio of two densities characterizes their differences. We consider the two-sample comparison problem through estimating the density ratio given i.i.d. observations from each distribution. We propose additive tree models for the density ratio along with efficient algorithms for training these models using a new loss function called the balancing loss. With this loss, additive tree models for the density ratio can be trained using several algorithms originally designed for supervised learning. First, they can be trained from an optimization perspective through boosting algorithms including forward-stage-wise fitting and gradient boosting. Moreover, due to the balancing loss function's resemblance to an exponential family kernel, it can serve as a pseudo-likelihood for which conjugate priors exist, thereby enabling effective generalized Bayesian inference on the density ratio using backfitting samplers designed for Bayesian additive regression trees (BART). This generalized Bayesian strategy enables uncertainty quantification on the inferred density ratio, which is critical for applications involving high-dimensional and complex distributions, as in such problems uncertainty given limited data can often be substantial. We provide insights on the balancing loss through its close connection to the exponential loss in binary classification and to the variational form of f -divergence, in particular that of the squared Hellinger distance. Our numerical experiments demonstrate the accuracy and computational efficiency of the proposed approach while providing unique capabilities in uncertainty quantification. We demonstrate the application of our method in a case study involving assessing the quality of generative models for microbiome compositional data.

1 Introduction

A vast range of applications involve comparing two groups of observations to assess their differences. The classical formulation of the two-sample comparison often involves parametric or semiparametric assumptions on the underlying distributions and focuses on testing the null hypothesis of no difference

with or without a given alternative in mind. However, this hypothesis testing perspective is often inadequate for most modern applications of two-sample comparison. Practitioners today typically also desire to learn the specific nature of the underlying difference. This problem lies at the core of numerous other modern statistical analyses and machine learning objectives.

For example, in large-scale biomedical studies involving the comparison of genetic measurements and various biomarkers between patients and controls, there is often no question that some types of two-sample differences do exist, and with a sufficiently large sample size, the null of no difference at all *will* be rejected. It is more helpful to specifically pinpoint what such differences are in order to help understand their biological meaning. Another timely application is the assessment of generative models. The key to assessing the quality of different models and algorithms for generating synthetic samples that imitate the real sampling distribution of the training data lies in deciphering the distributional difference between the real sampling distribution and that induced by the generative models, which is essentially a two-sample comparison problem. Some generative models, such as generative adversarial networks (GANs) (Goodfellow et al., 2014), essentially iteratively apply two-sample comparison and use the estimated misfit between the two distributions to sequentially improve the generative model. Two-sample comparison is also a quintessential problem in causal inference, in which consistent estimation of treatment effects often relies on correctly adjusting for the difference in the covariate distributions between the treated and the control groups.

Our focus here is on carrying out two-sample comparison in a nonparametric fashion through estimation rather than hypothesis testing, using the density ratio function as the functional “statistic” of interest for characterizing two-sample differences. The density ratio fully summarizes how two distributions differ across the sample space, and thus allows one not only to carry out hypothesis testing but also to identify the nature of the difference as well. If, for example, the estimated density ratio deviates “significantly” away from 1 on parts of the sample space, it allows us to draw statistical conclusions regarding whether, where, and how the two distributions differ. At the same time, the notion of “significant” deviation will require some form of uncertainty quantification for the inferred density ratio, which will become available under our formulation.

One may reasonably raise the concern that nonparametric density ratio learning is simply “too hard” for complex, high-dimensional data because density estimation itself in such settings is already a challenging problem. Why then would one attempt an even harder problem of learning the ratio of two densities? Though it might appear counter-intuitive, we argue that density ratio estimation (DRE) is in fact a much easier problem than density estimation in most modern applications. A density by definition is always a density ratio, with the denominator being the corresponding base measure against which the density is computed. The typical base measure, for example the Lebesgue measure or the uniform density in continuous cases, is generally chosen out of mathematical convenience and lack of prior knowledge, without taking any account of the dataset at hand (other than that the observations are continuous). This base measure generally does not resemble any sampling distribution in high-dimensional or otherwise complex problems. When good reliable knowledge of the

sampling distribution does exist, one would be in the much simpler classical setting of a “goodness-of-fit” problem. In contrast, in most applications of two-sample comparison, the two distributions are often quite similar to each other and can serve as a “baseline of reference” for each other. As such, the density ratio between these two samples then is often much simpler than the underlying densities (i.e., their ratios with respect to the Lebesgue measure).

We believe this explains a well-known observation in the DRE literature, that though estimating a density ratio can be done by first separately estimating the two densities and then computing their ratios based on the density estimates, it is usually more effective to adopt a method directly aimed at the density ratio, especially when the difference exists only in a small subset of the sample space or in a subset of the dimensions. Several authors have adopted this perspective and proposed methods directly targeting the density ratio. Some approaches include kernel-based methods (e.g. Sugiyama et al., 2007b; Kanamori et al., 2009; Hido et al., 2011; Liu et al., 2013; Yamada et al., 2013) and more recently neural network-based methods (Kato and Teshima, 2021).

Beyond the stand-alone two-sample comparison problem which is our focus herein, DRE has also been applied as a component in various learning methods in which two-sample comparison arises as a sub-problem directly or indirectly. A far-from-exhaustive list includes the estimation of the mutual information (Suzuki et al., 2009a,b), conditional density estimation (Sugiyama et al., 2010), covariate shift correction (Shimodaira, 2000; Sugiyama et al., 2007a; Reddi et al., 2015; Stojanov et al., 2019), outlier detection (Hido et al., 2011; Kato and Teshima, 2021), causal inference (Uehara et al., 2020), and change point detection (Kawahara and Sugiyama, 2009; Liu et al., 2013; du Plessis et al., 2015). Additionally, estimating density ratios has been utilized in Markov Chain Monte Carlo (MCMC) for intractable likelihoods (Kaji and Ročková, 2023).

We list several desiderata for learning the density ratio and discuss how we aim to achieve them. First, the model or function class representing the density ratio should be flexible enough to effectively approximate complex forms of the underlying truth. It should scale well with both sample size and in dimensionality. To these ends, we propose a class of density ratio learners based on additive tree ensembles (see e.g., Friedman et al., 2000; Hastie et al., 2009). Additive tree ensembles are a natural candidate for the density ratio problem, because of their success in classification problems. In fact, in the machine learning literature, a widely used technique to learn the density ratio between two samples is the so-called “density-ratio trick” (Sugiyama et al., 2012; Durkan et al., 2020; Thomas et al., 2022), which involves first fitting a binary classifier to the two samples, and then, based on the estimated posterior odds of the sample label, computing the density ratio. Additive tree boosting such as AdaBoost is among the most effective methods for binary classification.

In contrast to this popular perspective, we hold that DRE should not and does not need to involve the indirect route of inverting a binary classifier based on additive tree ensembles, but can instead be directly learned from the latter. As we will show, the resulting estimates are often substantially more accurate than what the density -ratio trick produces, especially when the sample size is unbalanced and/or the two-sample difference is local. In these scenarios, losses designed for binary classification

are poor proxies for learning the density ratio.

In terms of computational strategies, we introduce two boosting algorithms for estimating the additive tree model on density ratios. We use an additive tree ensemble as the function class for approximating the density ratio, by adding tree-based weak learners. The first algorithm is based on forward-stage-wise fitting (Hastie et al., 2009) and it operationally resembles AdaBoost. In each iteration, the observations are weighted according to the discrepancies between the current estimate and the actual responses, so that in each step we can fit a new weak learner that focuses on observations with large discrepancies. This algorithm sequentially and greedily minimizes the balancing loss through fitting a single-tree piecewise constant approximation to the density ratio of the weighted samples. The second algorithm follows the general paradigm of gradient boosting (Friedman, 2001).

These algorithms inherit important advantages of supervised tree boosting — they can be implemented at a small computation cost, and at the same time achieve good numerical performance, especially when the difference lies in a marginal distribution of a subset of the variables. One can incorporate regularization to avoid overfitting effectively by making the contribution of each base learner weak through a small learning rate, following the standard approach in supervised boosting (Hastie et al., 2009; Friedman, 2001).

The second desideratum is to attain uncertainty quantification for the estimated density ratio, thereby allowing statistical inference to proceed. This aspect has mostly been ignored in the existing literature on DRE. One exception is Bayesian nonparametric models for the density ratio using a single tree model (Ma and Wong, 2011; Soriano and Ma, 2017). While they provide a means to examine posterior uncertainty in a fully Bayesian manner, piecewise-constant functions represented by single trees of controlled complexity are very restrictive and therefore inadequate for approximating complex density ratios. Additive trees substantially enrich the class of functions, but they do not allow a simple likelihood formulation for modeling density ratios, and consequently, fully Bayesian uncertainty quantification for this function class is challenging. To overcome this, we propose a generalized Bayesian approach (Bissiri et al., 2016) using the balancing loss to construct a pseudo-likelihood for this model class. Interestingly, we show that, due to the resemblance of the balancing loss to an exponential family kernel, there exists a natural conjugate prior for the model parameters under the pseudo-likelihood, which allows standard sampling strategies for BART models (Chipman et al., 2010) to be directly adopted for sampling the Gibbs posterior on the density ratio.

The remainder of the paper is organized as follows. In Section 2 we start by introducing the balancing loss for learning the density ratio and highlight its connection to the variational form of the squared Hellinger distance and to the exponential loss for binary classification. We then introduce an additive tree model for the (log) density ratio along with two boosting algorithms for fitting this model based on forward stage-wise fitting and gradient boosting, respectively. In Section 3, we introduce a generalized Bayesian inference framework that uses the balancing loss as a (log) pseudo-likelihood and show that one can accomplish Bayesian backfitting sampling on the model using standard algorithms for BART by exploiting the analogy of the pseudo-likelihood to an exponential family. In Section 4,

we evaluate the performance of the proposed methods in comparison with the existing approaches in a few simulation settings, followed by a case study that assesses and comparing multiple generative models for microbiome compositions in Section 5. We give concluding remarks in Section 6.

2 Method

2.1 The balancing loss for density ratio learning

Let P and Q be unknown probability measures defined on the common sample space denoted by Ω . We focus on the case where Ω is a d -dimensional Euclidean space. We assume that the two measures P and Q admit density functions with respect to the Lebesgue measure μ and they are denoted by p and q , respectively. Our goal is to estimate the unknown density ratio p/q based on two i.i.d. samples.

Let r denote an estimate of the density ratio. In the following discussion, we assume that r is positive μ -almost everywhere. To introduce an algorithm for optimizing r , we define a loss function called the balancing loss based on the following fact: If r is equal to the true density ratio p/q , then for any measurable subset $B \subset \Omega$, we have

$$\int_B r^{-1/2} p d\mu = \int_B r^{1/2} q d\mu = \int_B \sqrt{pq} d\mu. \quad (1)$$

When $B = \Omega$, the whole sample space, this corresponds to the affinity between p and q . The first equation implies that if we weight the two samples respectively with $r^{-1/2}$ and $r^{1/2}$, their probability over any measurable set B becomes equal. In this sense, we say that the two samples are “balanced”. Motivated by this observation, we introduce the notation $w = r^{1/2}$ to denote the *balancing* function, which is intended to approximate the square root of the density ratio $\sqrt{p/q}$. We then consider the following *balancing* loss function:

$$l(w) = \mathbb{E}_p[w^{-1}] + \mathbb{E}_q[w].$$

In practice, suppose we observe i.i.d. draws from p and q :

$$x_1^{(0)}, \dots, x_{n_0}^{(0)} \sim p, \quad x_1^{(1)}, \dots, x_{n_1}^{(1)} \sim q.$$

Then the finite-sample version of the balancing loss is defined by

$$l_n(w) = \frac{1}{n_0} \sum_{i=1}^{n_0} w^{-1}(x_i^{(0)}) + \frac{1}{n_1} \sum_{i=1}^{n_1} w(x_i^{(1)}),$$

where $n = n_0 + n_1$ indicates the total number of observations.

2.2 Connections to existing concepts in statistical learning

While the design of the balancing loss may appear *ad hoc* at first, we next show that it can be naturally motivated from two well-established perspectives in machine learning.

2.2.1 Connection 1: the “density ratio trick” based on binary classification

The first perspective is related to a common technique widely adopted in the machine learning community for estimating density ratios, often referred to as the “density-ratio trick”, which involves turning the problem into a supervised, binary classification task on the two group labels (Sugiyama et al., 2012; Durkan et al., 2020; Thomas et al., 2022). It involves inverting a binary classifier to compute the density ratio. We show that the balancing loss arises naturally in this context as a variant of the exponential loss widely used in this context, but only the balancing loss targets the density ratio directly and thus is more robust than the density ratio trick against scenarios such as when the two sample sizes are unbalanced and/or the two-sample differences exist locally in a small subset of the sample space. These will also be validated experimentally later in our numerical examples where a direct comparison with the density ratio trick will be provided.

The balancing loss can be seen as a modification of the exponential loss, which is used for classification with the AdaBoost, described in Friedman et al. (2000). To see this, we suppose that, in generating the two samples, one first randomly decides which sample to draw the observation from with equal probability. That is, one first draws a random variable y that takes 1 and -1 with a 50-50 chance. Given y one generates the corresponding sample x from P if $y = 1$ and from Q if $y = -1$, respectively. Then it is straightforward to show that

$$\mathbb{E}_p[w^{-1}] + \mathbb{E}_q[w] \propto \mathbb{E}[e^{-yF}],$$

where $F = \log w$, and the expectation in the latter is taken with respect to the joint distribution of x and y . What we have on the right-hand side is exactly the exponential loss (Friedman et al., 2000; Hastie et al., 2009).

We note that the exponential loss used in AdaBoost in fact integrates y with respect to its marginal distribution from the data rather than using a 50-50 split. Because the population minimizer for the AdaBoost is the log posterior odds between the two samples (Friedman et al., 2000), which is the product of the density ratio and the prior odds, one may wonder then why the original AdaBoost cannot suffice for learning density ratios since one can simply multiply by a constant (i.e., the ratio of the proportion of the two samples) to get an estimate of the density ratio. The main reason is that, by weighting the loss using the marginal proportion of the two samples, vanilla AdaBoost prioritizes classification accuracy over density ratio estimation; this can be most clearly demonstrated when there are parts of the sample space in which one of the samples is much more abundant than the other, which can occur when the sample sizes are very different or when the two sample densities have different supports or tail behaviors. Such cases are in fact quite common in multivariate applications, and numerical evaluations will be provided in Section 4.

Connection 2: The variational form of the squared Hellinger distance

The design of the balancing loss can also be motivated from the perspective of estimating the an f -divergence between p and q . In particular, in this section we show that the balancing loss turns out

to be exactly equivalent to the variational form of one particular f -divergence, namely the squared Hellinger distance.

For a given convex function f , the general f -divergence is defined as $D_f(P||Q) := \int f(\frac{p}{q})dQ$. It is known (Rényi, 1961; Csiszár, 1964; Ali and Silvey, 1966; Nguyen et al., 2010; Polyanskiy and Wu, 2025) that the dual form can be written as an optimization problem with respect to a functional class \mathcal{F} mapping from \mathcal{X} to \mathbb{R} ,

$$D_f(P||Q) \geq \sup_{g \in \mathcal{F}} \int [gdP - f^c(g)dQ] \quad (2)$$

where f^c is the conjugate dual function of f , defined as $f^c := \sup_{u \in \mathbb{R}} \{uv - f(u)\}$. The dual objective is referred to as the variational form of the f -divergence. In the case of the squared Hellinger divergence, $f(u) = \frac{1}{2}(\sqrt{u} - 1)^2$, and the dual objective is $\sup_{g < \frac{1}{2}} \left\{ \mathbb{E}_P[g(X)] - \mathbb{E}_Q \left[\frac{g(X)}{1-2g(X)} \right] \right\}$ with the optimum value $g^* = \frac{1}{2} - \frac{1}{2}\sqrt{\frac{q}{p}}$, based on a direct application of Lemma 1 in Nguyen et al. (2010). Now let $w = (1 - 2g)^{-1}$, the variational form for the squared Hellinger divergence becomes

$$\sup_{w > 0} \left\{ 1 - \frac{1}{2} \int w^{-1}pd\mu - \frac{1}{2} \int wqd\mu \right\} \quad (3)$$

which is clearly equivalent to minimizing the balancing loss. In other words, learning the density ratio by minimizing the balancing loss is essentially estimating the squared Hellinger distance using its variational form. Based on the known minimizer of the variational form, the minimizer of the balancing loss is $w^* = \sqrt{p/q}$. Hence, learning the density ratio can be achieved by minimizing the balancing loss.

Beyond these two additional motivations for the balancing loss, we will see later that the symmetry of the balancing loss, in w vs w^{-1} and p vs q , will become handy when designing a generalized Bayesian framework to carry out inference on additive tree models.

2.3 Additive tree models and boosting

Given the close relationship between density ratios and posterior odds, the latter of which can be estimated using supervised tree boosting with additive tree models, it is natural to consider the class of additive tree models as a promising candidate for approximating the density ratio. We thus consider from now on fitting additive tree models to the density ratio under the balancing loss.

We begin with a non-Bayesian approach that aims to find a (functional) point estimate of the density ratio by optimizing the finite-sample version of the balancing loss. The resulting training algorithms are very similar to those used in supervised tree boosting. Before introducing the algorithms, we describe the additive tree model. We consider a model for the log-balancing weight $\log w$ in the form

$$\log w = \sum_{k=1}^K f_k \quad (4)$$

where each base learner f_k is a piecewise constant function defined on the leaf partition of the sample space given a tree T_k with leaf node parameters $\beta_k = \{\beta_k(A)\}_{A \in T_k}$ and written as

$$f_k = \sum_{A \in T_k} \beta_k(A) \mathbf{1}_A. \quad (5)$$

Under this model, we are now presented with the following optimization problem:

$$\min_{\{f_k\}} l_n(w) = \min_{\{\beta_k, T_k\}} \frac{1}{n_0} \sum_{i=1}^{n_0} w^{-1}(x_i^{(0)}) + \frac{1}{n_1} \sum_{i=1}^{n_1} w(x_i^{(1)})$$

Next, we introduce two algorithms for fitting the above model under the balancing loss. These are direct counterparts of two different approaches to fitting additive trees in supervised learning problems. The first corresponds to a forward-stagewise (FS) algorithm based on greedy steepest descent on the space of single-tree-based piecewise-constant functions; the other corresponds to Friedman (2001)'s gradient boosting (GB) algorithm. In practice, these algorithms typically produce estimates that are very similar to each other, and so one could just adopt the simpler GB algorithm, but because the details of the FS algorithm shed more light on what constitutes effective function approximators for the density ratio under the balancing loss, we believe they are worthy of elaboration here.

Algorithm 1: A forward-stagewise algorithm

The following proposition characterizes the optimal single tree fit in each iteration of a forward-stagewise algorithm, which takes K steps of iterative fitting and in each step k finds the optimal fit of f_k that minimizes the balancing loss. Its proof is provided in Supplementary Materials A.

Proposition 2.1. *Suppose w_{k-1} is the estimate of w after $(k-1)$ steps of fitting. Then in the k th step, the loss is minimized by $\log w_k = \log w_{k-1} + f_k$ when the following conditions are satisfied by f_k :*

1. Let $P_k|_{T_k}$ and $Q_k|_{T_k}$ be discrete distributions with their probability masses indexed by $A \in T_k$ such that

$$P_k|_{T_k}(A) \propto \int_A w_{k-1}^{-1} p d\mu, \quad Q_k|_{T_k}(A) \propto \int_A w_{k-1} q d\mu.$$

Then T_k is a partition structure that maximizes the Hellinger distance

$$H(P_k|_{T_k}, Q_k|_{T_k}) = \frac{1}{\sqrt{2}} \sqrt{\sum_{A \in T_k} (P_k|_{T_k}(A) - Q_k|_{T_k}(A))^2}.$$

2. For each $A \in T_k$,

$$e^{\beta_k(A)} = \sqrt{\frac{\int_A p w_{k-1}^{-1} d\mu}{\int_A q w_{k-1} d\mu}}.$$

Remark 1: If the balancing weight is correctly estimated, it achieves the symmetry between the two expectations in the loss in that $\mathbb{E}_p[w^{-1}] = \mathbb{E}_q[w]$, and we can impose this condition as a restriction or

regularization on the estimator so that it does not focus on minimizing only one expectation out of the two. As justification, Proposition 2.1 implies that the balancing loss can be improved by multiplying the current estimate w_k by a constant (c , say) such that $\mathbb{E}_p[(cw_k)^{-1}] = \mathbb{E}_q[cw_k]$ (see Supplementary Materials A for details). Based on this discussion, we introduce this correction step in the boosting algorithms.

Remark 2: Given the connection between the balancing loss and the variational form of the Hellinger divergence, it is not surprising that the “optimal” single-tree in each iteration corresponds to the partition that maximizes the corresponding discretized approximation of the Hellinger divergence.

As in tree-based predictive models, searching for the exact optimal tree in each step is often not computationally tractable for multivariate data. Instead one can adopt a greedy, coarse-to-fine algorithm in which we iteratively choose a single cut point at each split of the tree T_k that achieves the steepest ascent in the Hellinger distance or the steepest ascent in the corresponding affinity. Specifically, when we consider splitting the current node A , we can search for the splitting rule such that for the child nodes A_l and A_r the following affinity is minimized:

$$\sqrt{P_{k|T_k}(A_l)Q_{k|T_k}(A_l)} + \sqrt{P_{k|T_k}(A_r)Q_{k|T_k}(A_r)}.$$

Algorithm 2: A gradient boosting algorithm

We can also introduce a gradient boosting algorithm (Friedman, 2001). To this end, note that the negative gradients of the empirical loss with respect to the additive estimand F are as follows:

$$-\frac{\partial l_n(w)}{\partial F(x_i^{(0)})} = -\frac{1}{n_0}e^{-F(x_i^{(0)})} = \frac{1}{n_0}w^{-1}(x_i^{(0)}) \quad \text{and} \quad -\frac{\partial l_n(w)}{\partial F(x_i^{(1)})} = \frac{1}{n_1}e^{F(x_i^{(1)})} = -\frac{1}{n_1}w(x_i^{(1)}),$$

which are the pseudo-residuals. One can then follow the recipe provided in (Friedman, 2001). Specifically, in each iteration of the algorithm we fit a regression tree to the pseudo-residuals by minimizing the squared error loss, that is, minimizing the variances of the gradients in the leaf nodes. We again adopt a coarse-to-fine greedy search and for each node A , we select the splitting rule with child nodes A_l and A_r that minimizes the variances. After constructing the tree, we obtain the optimal values of the node parameters, which are already given by Proposition 2.1.

Regularization strategies

As for supervised problems, the success of tree boosting under the two algorithms above requires each base learner to be weak in the sense that it extracts only a small amount of structure in the density ratio function. Similar to supervised boosting, we can regularize the contribution of each learner to the estimate by introducing a learning rate denoted by $\nu \in (0, 1]$. If the current estimate is w_{k-1} and the optimal learner obtained in the k th step is f_k , we can combine them as follows:

$$\log w_k = \log w_{k-1} + \nu f_k.$$

It is known that smaller values of the learning rate ν lead to better generalization performance in both supervised learning (Friedman, 2001; Hastie et al., 2009) and unsupervised learning (Awaya and Ma, 2024). Accordingly, in our implementation, we follow them by setting ν to, for example, 0.01.

An additional, complementary strategy for regularization is to introduce a restriction on the size of trees to avoid constructing overly complicated partition structures, so we set the maximum resolution (depth) of the trees to be, for example, between 4 and 6. Finally, the number of trees in the ensemble also needs to be carefully selected. We find that choosing this number via cross-validation yields satisfactory performance.

3 Generalized Bayesian inference on additive trees for density ratios

3.1 Balancing loss as a pseudo-likelihood

Tree boosting only offers point estimates for the density ratio function, without providing any uncertainty associated. To achieve uncertainty quantification for the density ratio, we can instead adopt a (generalized) Bayesian strategy (Bissiri et al., 2016) to learning the density ratio. Specifically, we define a pseudo-likelihood using the finite-sample loss $l_n(w)$, that is

$$L_{n,\tau}(w) = \exp(-n\tau l_n(w)),$$

where $\tau > 0$ is a “temperature” parameter. Then, given the prior distribution of w , $\pi_0(w)$, the posterior distribution of w is defined as

$$\pi(w) \propto \pi_0(w)L_{n,\tau}(w),$$

3.2 Conjugate prior specification

Next we describe prior specification on w for efficient MCMC and a data-driven approach for setting the value of τ . Recalling our model introduced in (4), we describe a Gibbs sampling strategy that iteratively samples the full conditional of each basis function f_k , given all the others. That is, how one may sample the node parameters $\beta_k(A)$ and the tree partition T_k that define f_k as in (5).

3.2.1 Updating leaf node parameters

To derive the full conditional for $\beta_k(A)$, we define the balancing weight with f_k subtracted:

$$\log w_{-k} := \log w - f_k.$$

The portion of the likelihood $L_{n,\tau}(w)$ that depends on $\beta_k(A)$ is given by

$$L_{n,\tau}(w) \propto \exp \left(-\zeta^{-1}\tau\gamma_k(A)^{-1} \sum_{x_i^{(0)} \in A} w_{-k}^{-1}(x_i^{(0)}) - (1 - \zeta)^{-1}\tau\gamma_k(A) \sum_{x_i^{(1)} \in A} w_{-k}(x_i^{(1)}) \right),$$

where $\zeta = n_0/n$ and $\gamma_k(A) = e^{\beta_k(A)}$. We note that this pseudo-likelihood resembles an exponential family kernel for $\gamma_k(A)$, and as such we adopt an inverse-Gaussian prior for $\gamma_k(A)$, which is conjugate to this kernel. Specifically, the prior $\text{InverseGauss}(\mu_k(A), \lambda_k(A))$ on $\gamma_k(A)$ takes the following form:

$$\begin{aligned} p(\gamma_k(A) = z \mid \mu_k(A), \lambda_k(A)) &= \sqrt{\frac{\lambda_k(A)}{2\pi z^3}} \exp\left(-\frac{\lambda_k(A)(z - \mu_k(A))^2}{2\mu_k(A)^2 z}\right) \\ &\propto \sqrt{\frac{\lambda_k(A)}{2\pi z^3}} \exp\left(-\frac{\lambda_k(A)}{2\mu_k(A)^2} z - \frac{\lambda_k(A)}{2z}\right). \end{aligned}$$

It is straightforward to see that the conditional posterior is analytically obtained in the form of $\text{InverseGauss}(\mu'_k(A), \lambda'_k(A))$, where

$$\mu'_k(A) = \sqrt{\frac{\lambda_k(A) + 2\zeta^{-1}\tau \sum_{x_i^{(0)} \in A} w_{-k}^{-1}(x_i^{(0)})}{\frac{\lambda_k(A)}{\mu_k(A)^2} + 2(1 - \zeta)^{-1}\tau \sum_{x_i^{(1)} \in A} w_{-k}(x_i^{(1)})}}, \quad \lambda'_k(A) = \lambda_k(A) + 2\zeta^{-1}\tau \sum_{x_i^{(0)} \in A} w_{-k}^{-1}(x_i^{(0)}). \quad (6)$$

We set $\mu_k(A)$ to 1 so that the induced marginal prior on $\log w$ is around 0 (more discussions are to be given at the end of this section). The precision parameter $\lambda_k(A)$ induces shrinkage toward the prior mean 1, as seen in the posterior mean $\mu'_k(A)$ given in Eq (6). We set $\lambda_k(A)$ according to the number of trees K :

$$\lambda_k(A) = \lambda_0 K,$$

where λ_0 is a hyperparameter. The prior value of $\lambda_k(A)$ is linear in K because the results in Whitmore and Yalovsky (1978) imply that the variance of $f_k(x)$ for each point x ($x \in \Omega$) is $O(K^{-1})$ under our model specification (see Supplementary Materials A for more details). This choice of $\lambda_k(A)$ is also analogous to the amount of shrinkage recommended for the BART model (Chipman et al., 2010). We set λ_0 to 5 as a default value in all of our numerical experiments.

Another consideration is that the inverse Gaussian distribution has an asymmetric shape, so it can also introduce skewness into the prior of the log-balancing weight $\log w$. To avoid this issue, we apply the inverse Gaussian prior to $\gamma_k(A)$ and $\gamma_{k,A}^{-1}$ alternately, that is,

$$\begin{aligned} \gamma_k(A) &\sim \text{InverseGauss}(1, \lambda_0 K) \quad (k: \text{ odd}), \\ \gamma_k(A)^{-1} &\sim \text{InverseGauss}(1, \lambda_0 K) \quad (k: \text{ even}). \end{aligned}$$

This ensures that the marginal prior of $\log w$ is exactly centered at 0 whenever the total number of trees K is even.

3.2.2 Tree priors and posterior updates on the trees

We adopt the standard Bayesian CART prior (Chipman et al., 1998) on the tree T_k as in BART (Chipman et al., 2010) and describe the prior on T_k in terms of a recursive partition process. Starting

from the full sample space as the root node, each node A in the tree with depth $\text{depth}(A)$ (which is 0 for the root) is further split with probability

$$a_T(1 + \text{depth}(A))^{-b_T}, \quad a_T \in (0, 1), b_T \in [0, \infty).$$

We set the hyperparameters to the widely used default choices as $a_T = 0.95$ and $b_T = 2$ (Chipman et al., 2010). When splitting the node, one of the d candidate dimensions of the sample space is selected with equal probability, and a cut point is selected uniformly over the range in that dimension. Following the standard recipe for BART (Chipman et al., 2010; Kapelner and Bleich, 2016; Sparapani et al., 2021), we update the tree T_k by using Metropolis-Hastings moves. The details of the tree updating moves are provided in Supplementary Materials B.

3.3 Tuning the temperature τ

In generalized Bayesian inference, the temperature parameter τ controls the strength of the loss-based likelihood for the balancing weight function w relative to the prior and significantly influences the resulting posteriors, including posterior variances and credible intervals. There is a growing body of literature on strategies for selecting the temperature parameter empirically. Some proposed methods include information matching (Holmes and Walker, 2017), calibrating frequentist coverage rates of credible intervals (Syring and Martin, 2019), and the SafeBayes algorithm (Grünwald and van Ommen, 2017). However, it is not straightforward to adapt these methods to the current context, where the task is unsupervised and the function of interest is an unknown, nonparametrically specified function.

Instead, we adopt a hierarchical Bayesian approach by placing a prior on the temperature τ , following Bissiri et al. (2016); Rigon et al. (2023). To this end, we add τ^n to the pseudo-likelihood so that the full conditional of τ is proportional to

$$\pi_0(\tau)\tau^n \prod_{i=1}^{n_0} \exp\left(-\zeta^{-1}\tau w^{-1}(x_i^{(0)})\right) \prod_{i=1}^{n_1} \exp\left(-(1-\zeta)^{-1}\tau w(x_i^{(1)})\right),$$

where $\pi_0(\tau)$ denotes the prior for τ . We adopt a conjugate prior $\pi_0(\tau)$, namely $\text{Gamma}(a_{0,\tau}, b_{0,\tau})$, so the full conditional of τ is $\text{Gamma}(a_{1,\tau}, b_{1,\tau})$, where

$$a_{1,\tau} = a_{0,\tau} + n, \quad b_{1,\tau} = b_{0,\tau} + nl_n(w).$$

The analytic form of the full conditional elucidates the role τ plays and justifies the data-dependent approach to tuning its value. Specifically, τ can be interpreted as a regularization parameter that penalizes poor overlap of the two samples. To see this, note that the full conditional mean of τ is $\frac{a_{0,\tau} + n}{b_{0,\tau} + nl_n(w)}$, so when the total sample size is large, the inverse of this quantity approximates the realized value of the loss $l_n(w)$. When the two samples have little overlap, for example, the estimated weights w^{-1} for the first group and w for the second group tend to be both small and close to zero, leading to a small $l_n(w)$ and thus a large τ . Conversely, when the samples have good overlap, the weights are closer to 1, yielding a larger $l_n(w)$ and a smaller τ . As an illustration, Figure 1 shows the

posterior distributions of τ under different levels of overlap under a simple simulation experiment. The observations ($n_0 = n_1 = 200$) are generated from the standard normal distribution, and the second group is mean-shifted by 1, 2, and 3, corresponding to decreasing levels of overlap. We can see that poorer overlap of the two samples leads to larger absolute values of $\log w$, along with larger values of τ corresponding to the smaller realized value of the loss $l_n(w)$.

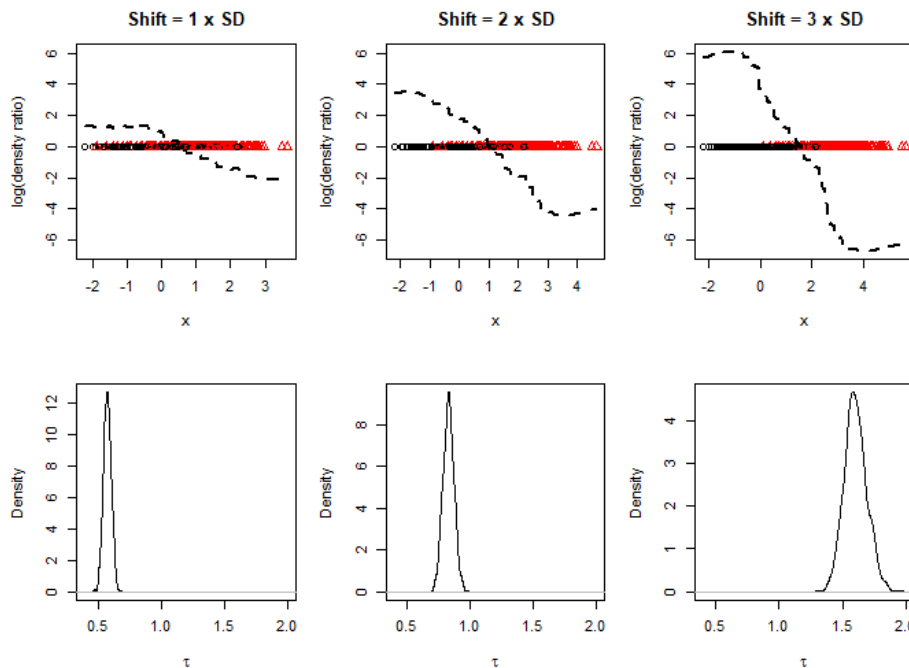


Figure 1: Posterior distributions of τ under different levels of overlap. Top row: The black and red points correspond to the two samples, and the dashed lines indicate the posterior means of the log-density ratios. Bottom row: The density functions of the posterior distributions of τ are shown.

4 Numerical Experiments

We conduct simulation experiments to evaluate the proposed methods—both tree boosting and Bayesian additive trees. We begin with scenarios involving bivariate distributions, and then consider higher-dimensional (20-dimensional) cases. We provide a comparison with several existing approaches. The first approach to be compared with is the “density-ratio trick” by inverting a binary classifier. In particular, we adopt AdaBoost as binary classification, as it uses the same class of additive tree ensembles to classify the two classes using essentially the exponential loss (Friedman et al., 2000). The difference between this approach and our boosting algorithms is essentially be due to the different loss functions employed. To apply the density-ratio trick, we first estimate the classification probabilities and then transform them into the density ratios by multiplying the sample size ratios. For implementation, we use the `ada` function provided in the R package `ada` (Culp et al., 2016). In

addition to the “density-ratio trick”, we also compare our methods with two popular kernel-based density ratio estimators, namely KLEIP (Sugiyama et al., 2008) and uLSIF (Kanamori et al., 2009), implemented with the R package `densratio` (Makiyama, 2019).

For boosting, we assess both the FS and the GB algorithms. The learning rate ν is set to 0.01, and the maximum resolution of each tree is set to 4. The optimal number of trees is selected with the 5-fold cross-validation with the maximum number allowed set to 1000. For a fair comparison, AdaBoost is implemented under the same tuning parameters. For the generalized Bayesian additive tree model, we set the size of the ensemble to 200, following the standard implementation of the BART (Chipman et al., 2010). The MCMC sampler is initialized with trees containing only root nodes, and the size of the burn-in and the posterior sample is set to 2000 and 1000, respectively. In both types of the proposed models, we introduce 31 equally spaced cut points in each dimension. Further details on the implementation are provided in Supplementary Materials C.

For each scenario, we evaluate the performance under two sample size settings: (i) $n_0 = n_1 = 5000$ (the “balanced” setting) and (ii) $n_0 = 9000, n_1 = 1000$ (the “unbalanced” setting). As a measure of accuracy, we use the following symmetrized squared mean error for the true density ratio r^* and the estimated ratio \hat{r} :

$$\frac{1}{2n_0} \sum_{i=1}^{n_0} \left(\log r^*(x_i^{(0)}) - \log \hat{r}(x_i^{(0)}) \right)^2 + \frac{1}{2n_1} \sum_{i=1}^{n_1} \left(\log r^*(x_i^{(1)}) - \log \hat{r}(x_i^{(1)}) \right)^2,$$

and for each setting we calculate the average MSE based on 50 simulated data sets.

4.1 2D simulations

We simulate data sets using the following three scenarios which represent different types of distributional differences between X_0 and X_1 :

1. Global shift

$$X_0 \sim N(\mu^{(0)}, I_2), \quad X_1 \sim N(\mu^{(1)}, I_2),$$

where $\mu^{(0)} = (-0.5, -0.5)'$ and $\mu^{(1)} = (0.5, 0.5)'$.

2. Local shift

$$X_0 \sim \frac{1}{5}N(\mu_1, \Sigma_1) + \frac{1}{5} \sum_{k=2}^5 N(\mu_k, \Sigma_k), \quad X_1 \sim \frac{1}{5}N(\mu_1 + \delta, \Sigma_1) + \frac{1}{5} \sum_{k=2}^5 N(\mu_k, \Sigma_k),$$

where $\delta = (0, 1)'$, and μ_k and Σ_k ($k = 1, \dots, 5$) are provided in Supplementary Materials C.

3. Local dispersion difference

$$X_0 \sim \frac{1}{3}N(\mu_1, \Sigma_1) + \frac{1}{3} \sum_{k=2}^3 N(\mu_k, \Sigma_k), \quad X_1 \sim \frac{1}{3}N(\mu_1, \Delta\Sigma_1) + \frac{1}{3} \sum_{k=2}^3 N(\mu_k, \Sigma_k),$$

where $\Delta = \text{diag}(0.36, 1)$, and μ_k and Σ_k ($k = 1, \dots, 3$) are provided in Supplementary Materials C.

The simulated data sets are visualized in Figure 2. The first scenario represents a global-scale difference between the two samples, whereas the second and third scenarios involve more localized discrepancies.

A comparison of the MSEs is provided in Table 1, and the results indicate that our proposed methods (the boosting and the Bayesian additive trees) generally outperform the other approaches. We note that, for the performance of the classification approach with AdaBoost, the MSEs increase substantially when comparing the balanced and unbalanced sample-size settings. This confirms the common observation that inverting a binary classifier to attain the density ratio loses its efficacy when the sample sizes are unbalanced. By contrast, the proposed balancing loss remains robust even with unbalanced sample sizes.

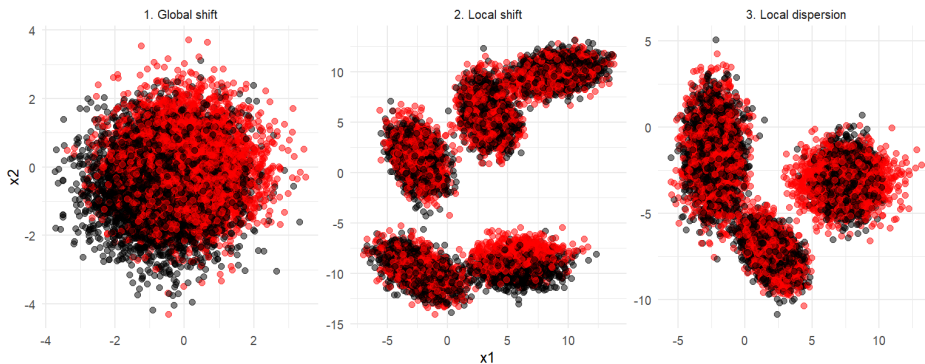


Figure 2: A representative sample of simulations generated from the three scenarios used for the two-dimensional experiments. The sample sizes, n_0 and n_1 , are both set to 5000.

Figure 3 compares the estimated log-density ratios in the local shift scenario with the balanced sample sizes ($n_0 = n_1 = 5000$). The estimated functions using the proposed methods successfully capture the local difference structure, and importantly, the log-density ratios are significantly positive or negative for many observations included in the mixture component that has the local shift difference. For example, in the plot of the 2.5% quantiles, we find observations with yellow/red colors, indicating that the log-density ratios are significantly larger than 0, mostly in the corresponding mixture component. Similar patterns are obtained for the other scenarios and sample size settings, and we provide their visualizations in Supplementary Materials D.

4.2 Higher-dimensional settings

In this experiment, we evaluate the performance of the density ratio estimation algorithms in higher-dimensional settings. We generate 20-dimensional observations based on a latent factor model. First, we simulate latent variables Z from 4-dimensional distributions, introducing the difference between

$n_0/(n_0 + n_1)$	Global Shift		Local Shift		Local Dispersion	
	0.5	0.9	0.5	0.9	0.5	0.9
GB	0.033 (0.001)	0.063 (0.002)	0.035 (0.001)	0.067 (0.002)	0.109 (0.002)	0.133 (0.005)
FS	0.036 (0.001)	0.071 (0.002)	0.035 (0.001)	0.070 (0.002)	0.111 (0.002)	0.133 (0.005)
BAT	0.012 (0.000)	0.031 (0.001)	0.049 (0.001)	0.067 (0.001)	0.116 (0.002)	0.131 (0.005)
DRT (AdaBoost)	0.199 (0.022)	2.715 (0.250)	0.151 (0.011)	3.289 (0.182)	0.173 (0.010)	2.692 (0.199)
KLIEP	0.151 (0.006)	0.159 (0.005)	0.301 (0.004)	0.316 (0.005)	0.305 (0.004)	0.308 (0.007)
uLSIF	1.348 (0.195)	0.470 (0.090)	0.412 (0.018)	0.390 (0.026)	0.130 (0.005)	0.199 (0.009)

Table 1: A comparison of the MSEs and their standard errors in the two-dimensional scenarios. The methods are GB (gradient boosting), FS (forward stagewise), BAT (Bayesian additive trees), DRT (density-ratio trick based on AdaBoost), and the two kernel-based methods KLIEP and uLSIF.

the two samples in this latent space, and then project them onto the 20-dimensional space as

$$\Lambda Z + \epsilon_i, \quad \epsilon_i \sim N(\mathbf{0}, (0.1)^2 I_{20}),$$

where Λ is a randomly generated orthonormal 20×4 matrix satisfying $\Lambda' \Lambda = I_4$. The distributions that the latent variables follow for the two groups, indicated by random variables Z_0 and Z_1 , are defined under the two scenarios described below.

1. Location Shift

$$Z_0 \sim \frac{4}{5}N(\mu_1, \Sigma_1) + \frac{1}{5}N(\mu_2, \Sigma_2), \quad Z_1 \sim \frac{4}{5}N(\mu_1 + \delta, \Sigma_1) + \frac{1}{5}N(\mu_2, \Sigma_2),$$

where $\delta = (1, 0, 0, 0)^T$. The parameters μ_k and Σ_k ($k = 1, 2$) are provided in Supplementary Materials C.

2. Dispersion Difference

$$Z_0 \sim \frac{4}{5}N(\mu_1, \Sigma_1) + \frac{1}{5}N(\mu_2, \Sigma_2), \quad Z_1 \sim \frac{4}{5}N(\mu_1, \Delta \Sigma_1) + \frac{1}{5}N(\mu_2, \Sigma_2),$$

where $\Delta = \text{diag}(0.5, 1, 1, 1)$. The parameters μ_k and Σ_k ($k = 1, 2$) are provided in Supplementary Materials C.

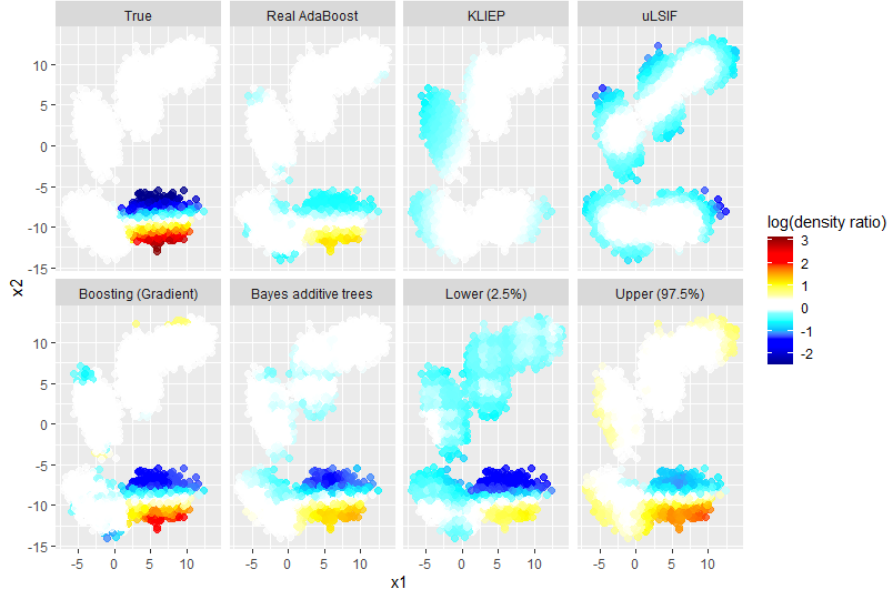


Figure 3: The estimated log-density ratios obtained from the algorithms considered in the two-dimensional examples for the local shift scenario ($n_0 = n_1 = 5000$). For the Bayesian additive model, the 2.5% quantiles and 97.5% quantiles of the log-density ratios evaluated pointwise are also displayed. The difference between FS and GB is minimal, so we present only the result for GB.

The orthonormal matrix Λ is generated using the `randortho` function in the R package `pracma` (Borchers, 2023).

Figure 4 shows the distribution of the first two latent factors, which account for the differences between the two groups, along with the corresponding true and estimated log density ratios. The latent factor model for the true densities represents a challenging case for density ratio estimation, particularly for tree-based methods that use axis-aligned partitions along the original dimensions of the sample space. Nevertheless, as shown in Table 2, the proposed methods still produce more accurate estimates, and the performance is robust to the unbalanced sample sizes. More importantly, in such challenging settings, uncertainty quantification becomes even more important to draw robust conclusions. The inferred density ratios must be gauged against appropriate measures of uncertainty to reach reliable inference. Our generalized Bayesian approach serves this need—the yellow/red regions in the lower quantiles and the blue points in the upper quantiles correspond to those falling outside the 95% credible bands, and these indeed align with the regions with true differences. Without this uncertainty quantification, the inferred different regions would have included much larger portions of the sample space across all of the estimates.

$n_0/(n_0 + n_1)$	Location Shift		Dispersion	
	0.5	0.9	0.5	0.9
GB	0.073 (0.001)	0.125 (0.002)	0.150 (0.003)	0.228 (0.005)
FS	0.076 (0.001)	0.136 (0.002)	0.158 (0.004)	0.237 (0.006)
BAT	0.059 (0.001)	0.115 (0.002)	0.171 (0.004)	0.202 (0.003)
DRT (AdaBoost)	0.237 (0.027)	3.858 (0.119)	0.151 (0.005)	3.031 (0.157)
KLIEP	0.611 (0.006)	0.609 (0.008)	0.547 (0.001)	0.548 (0.001)
uLSIF	3.379 (0.074)	3.621 (0.089)	0.546 (0.001)	0.547 (0.001)

Table 2: A comparison of the MSEs and their standard errors in the 20-dimensional scenarios. The methods are GB (gradient boosting), FS (forward stagewise), BAT (Bayesian additive trees), DRT (density-ratio trick using AdaBoost), and the two kernel-based methods KLIEP and uLSIF.

5 Assessing the quality of synthesized microbiome compositions

In recent years, various generative models have been introduced to imitate the sampling mechanisms of various complex biomedical data. In particular, several approaches have been proposed for generating microbiome compositions (Sankaran et al., 2025). A common need is to assess the quality of the synthetic samples drawn from these models by comparing them with the actual observed data. We apply our two-sample comparison framework to synthetic samples simulated from different generative models and the corresponding observed samples, thereby assessing the quality of data generation in these models.

The real microbiome data are obtained from the open-source Curated Metagenomic Data (Parsoli et al., 2017), available as the R package `curatedMetagenomicData`. We focus on the relative abundance data and apply the following subsetting rules: removing samples whose microbial relative abundance does not sum up to 1 (i.e., ≥ 0.99); then, keep taxa with average relative abundance $\geq 0.1\%$; among those taxa, keep only samples that have zeros in fewer than 10% of taxa and whose mean abundance is at least the overall average. After subsetting, each row contains 123 columns of species-level relative abundance. We use one of the largest studies, the IBDMDB dataset (Lloyd-Price et al., 2019) in the database, as the data of interest. (The samples are in fact collected at multiple time points for each given subject, but the longitudinal nature of the data is important for scientific analysis but could be ignored for the purpose of this demonstration since we will only be focusing on

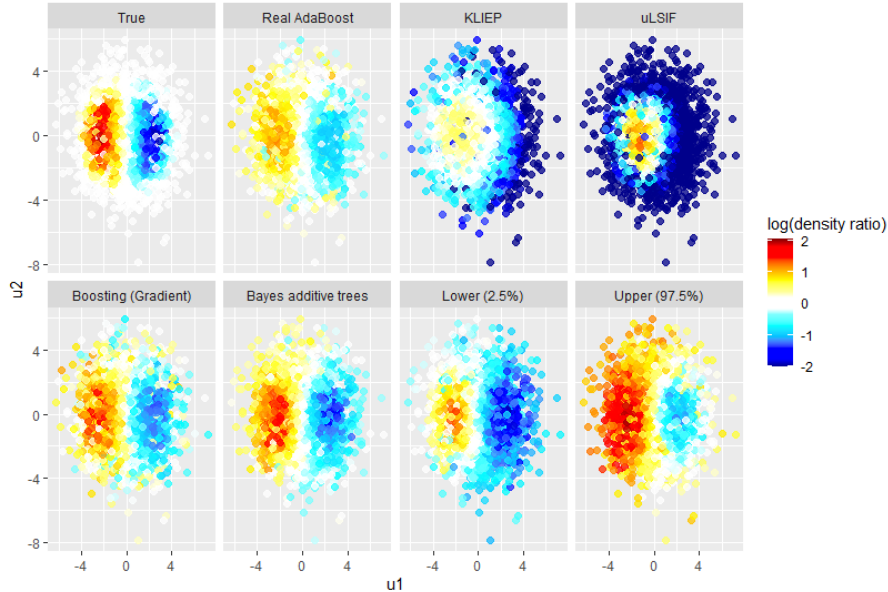


Figure 4: A comparison of the true log-density ratios and the estimated ratios projected onto the space of the latent variables (z_1, z_2) , for the location shift scenario ($n_0 = n_1 = 5000$). The difference in the results for FS and GB is minimal, so we present only the result for GB.

assessing how well generative models can approximate the marginal distribution of the samples.) We split the data into training ($n = 1166$) and testing ($n = 292$) sets. The generative models are trained using the training data, and the testing data are used in the follow-up two-sample comparison with the synthetic samples. We include various popular generative models, including both classical parametric models and state-of-the-art deep neural network-based models. The parametric models considered are the Dirichlet model (Holmes et al., 2012; La Rosa et al., 2012) and the Dirichlet tree model (Dennis III, 1991; Wang and Zhao, 2017; Mao and Ma, 2022). The nonparametric generators based on neural networks include continuous normalizing flows via conditional flow matching (Lipman et al., 2022; Tong et al., 2023, ICFM) (code available at <https://github.com/atong01/conditional-flow-matching>), and a generative adversarial network model called MB-GAN (Rong et al., 2021) (code available at <https://github.com/zhanxw/MB-GAN>), which is tailored for microbiome data generation. Our objective here is not to argue which model is better than others, as such judgments are context-dependent and require more careful tuning of each model. Rather, we aim to simply provide an example that density ratio-based two-sample comparison can provide insights into how various generative models can be gauged given the observations that they generate.

The PCoA plots based on the Bray-Curtis distance (Bray and Curtis, 1957) in Figure 5 provide a low-dimensional visualization for comparing the generated sample with the train/test sample. These plots clearly show that the parametric generators (Dirichlet and Dirichlet-Tree) have less coverage of the support than the train/test sample, while the two neural network-based approaches perform better in this regard. However, it is difficult to further differentiate the quality of the two neural

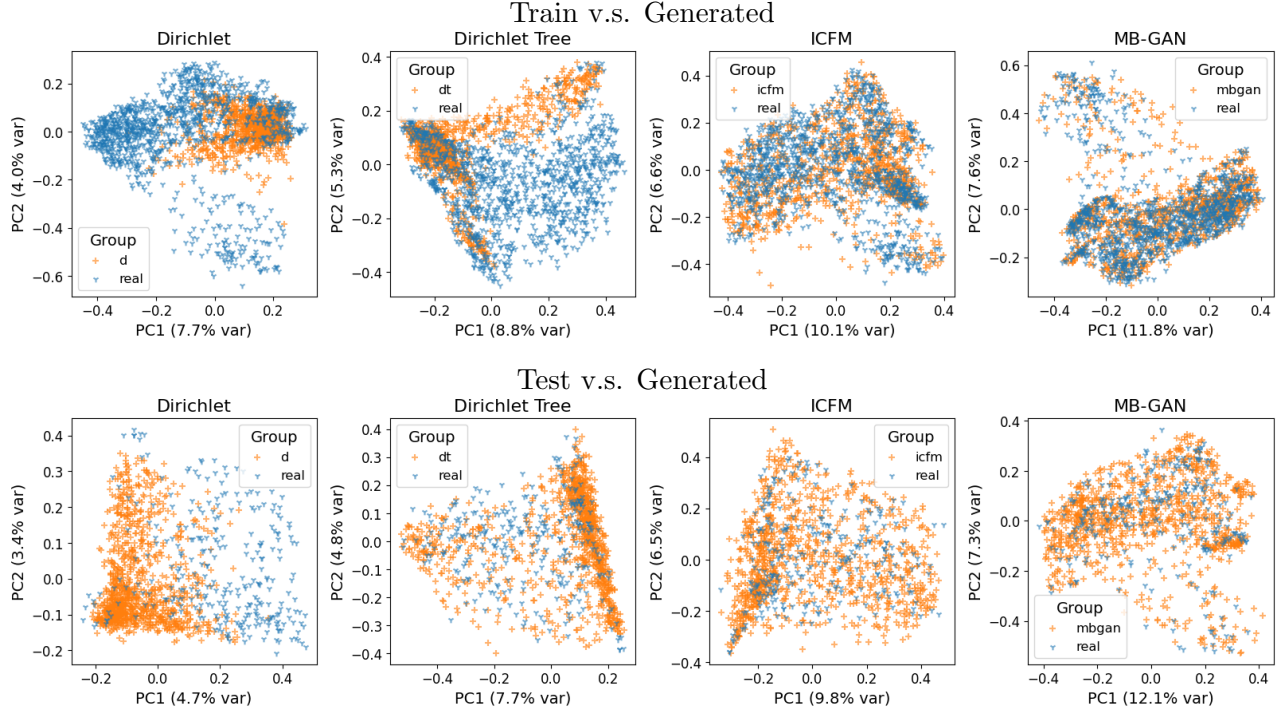


Figure 5: Principal Coordinates Analysis (PCoA) plots based on Bray-Curtis distance between samples. The blue and orange points represent the real sample and the generated sample, respectively. The first row presents the training sample vs the generated sample, and the second row presents the test sample vs the generated sample.

network-based generators based on such visualization.

We apply the generalized Bayesian additive trees and obtain a posterior sample of the density ratio evaluated at each of the real and the synthetic samples. We then compute the posterior mean along with a pointwise 95% credible band for the density ratio, as shown in Figure 6 (training sample vs synthetic sample) and Figure 7 (testing sample vs synthetic sample). The color indicates the estimated (log) density ratio. The estimated density ratios in both Figures 6 and 7 provide a clear contrast of the generation quality compared to the true sample. The estimated log-density ratio for the MB-GAN-generated sample versus the real sample is close to 0 across the support. The credible bands provided by our proposed method offer uncertainty quantification for the density ratio, demonstrating that 95% of the posterior mass of the log density ratio comfortably covers 0 over most of the sample space, which is not observed for the parametric models and ICFM.

6 Conclusion

We have introduced a new approach to learning the density ratio between two i.i.d. samples using an additive tree model as the function class. We showed that a new loss function called the balancing

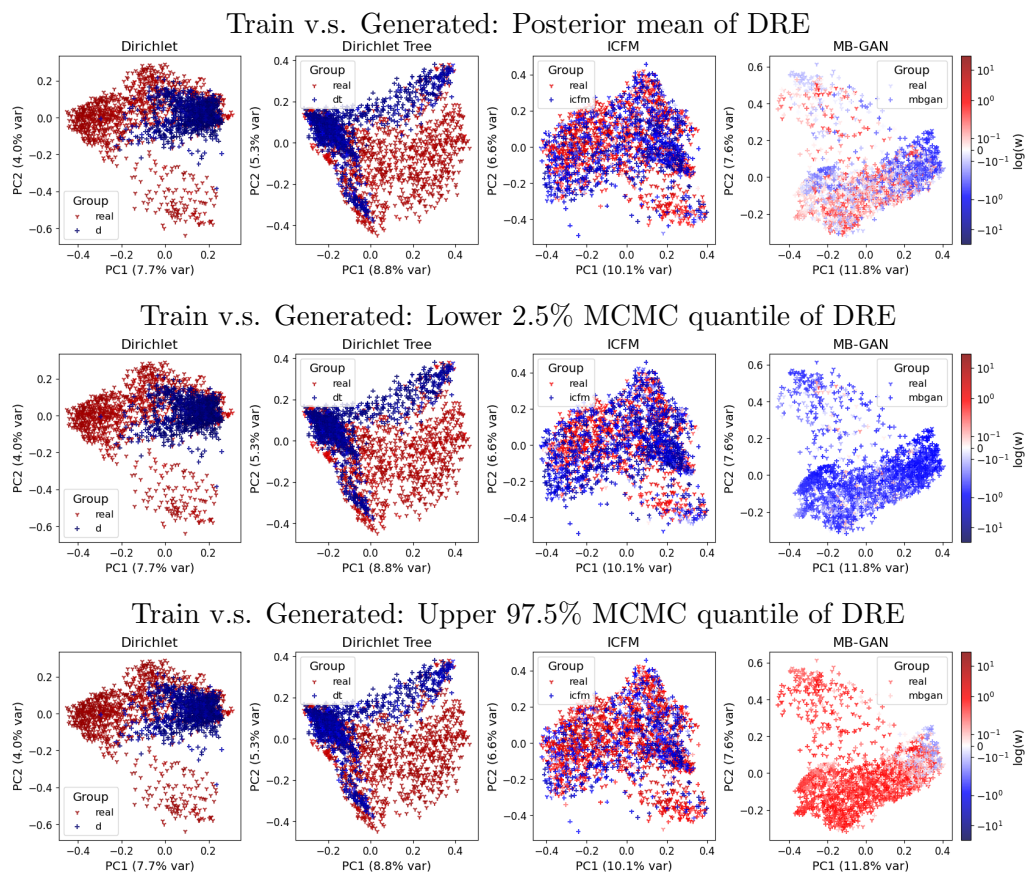


Figure 6: PCoA plots colored by the density ratio estimates of the training sample density over the generated sample density, along with the 2.5% and 97.5% credible bands.

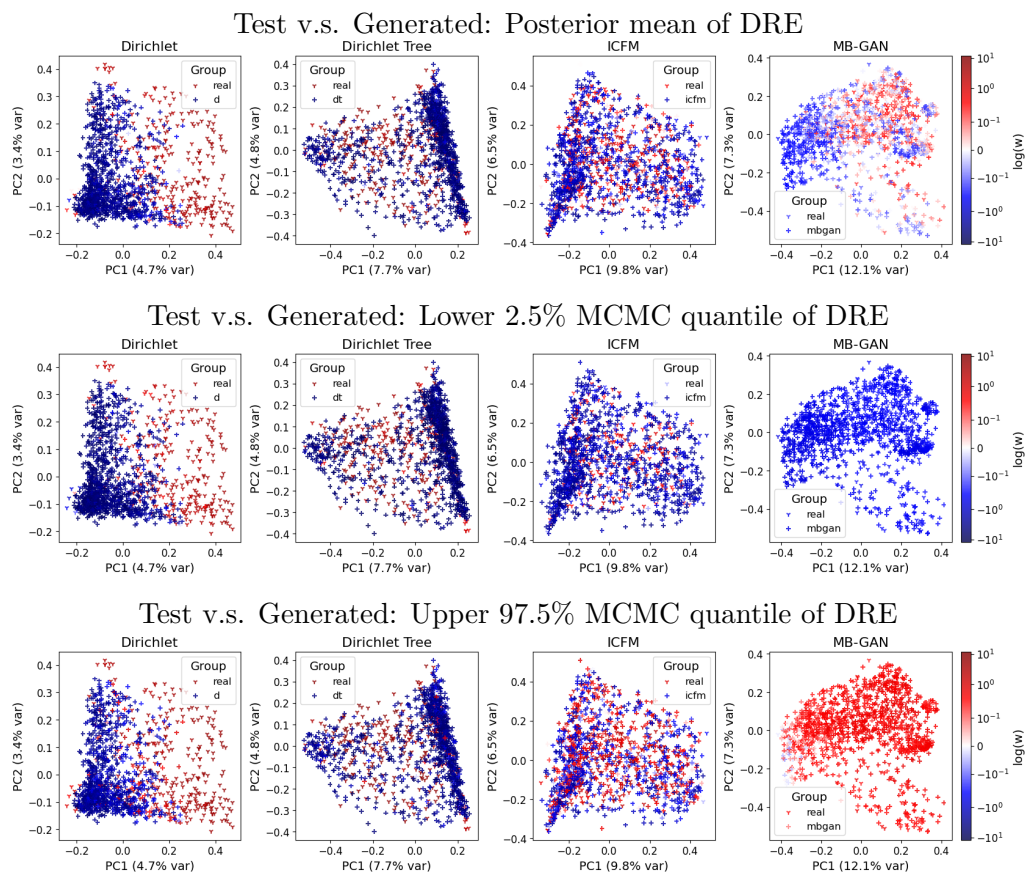


Figure 7: PCoA plots colored by the density ratio estimates of the testing sample density over the generated sample density, and the 2.5% and 97.5% credible bands.

loss can be highly effective in learning the density ratio based on this function class. Not only does it provide effective boosting algorithms to attain functional (point) estimates, but it also provides a convenient means to generalized Bayesian inference on the density ratio, attaining uncertainty quantification which can be critical in challenging problems where the uncertainty in the learned density ratio can be substantial. The training algorithms we presented, both for boosting and for generalized Bayesian learning, are only minor modifications of their counterparts widely used in supervised learning based on this model class, and so their implementation would involve only minor adjustments to existing software for boosting and BART models.

Additive tree models do have their limitations. In particular, they use axis-aligned partitions and therefore can sometimes be less effective at capturing high-order interactions, and they generally do not perform well with very high-dimensional data, i.e., those involving more than a few hundred dimensions. In such scenarios, an effective strategy is to couple the tree-based approaches with strategies for learning effective representations of the data. Examples of such representations might include low-dimensional subspace assumptions (e.g., manifolds) or other highly non-linear embeddings through state-of-the-art neural network-based encoders. Even in such cases, we believe that learning the density ratio between two samples is a worthy objective and will typically be easier to achieve than learning the density of each of the two samples *per se*.

Software

We have implemented an R package `BATTS` for the proposed boosting and Bayesian additive tree algorithms, and it is available at <https://github.com/MaStatLab/BATTS>. R code for reproducing the numerical experiments is also provided at https://github.com/MaStatLab/BATTS_experiments.

Acknowledgment

This research is funded in part by NIGMS grant R01-GM135440 and NSF grant DMS-2152999. Part of the research was completed when LM and YX were at Duke University. NA's research is supported by the Japan Society for the Promotion of Science KAKENHI (grant numbers: 25K16618, 24H00142, and 25H00546). The authors thank Dr. Ganchao Wei for preprocessing the IBDMDB data and generating the synthetic samples.

References

Syed Mumtaz Ali and Samuel D Silvey. A general class of coefficients of divergence of one distribution from another. *Journal of the Royal Statistical Society: Series B (Methodological)*, 28(1):131–142, 1966.

- Naoki Awaya and Li Ma. Unsupervised tree boosting for learning probability distributions. *Journal of Machine Learning Research*, 25(198):1–52, 2024.
- Pier Giovanni Bissiri, Chris C Holmes, and Stephen G Walker. A general framework for updating belief distributions. *Journal of the Royal Statistical Society. Series B, Statistical methodology*, 78(5):1103, 2016.
- Hans W. Borchers. *pracma: Practical Numerical Math Functions*, 2023. URL <https://CRAN.R-project.org/package=pracma>. R package version 2.4.4.
- J Roger Bray and John T Curtis. An ordination of the upland forest communities of southern wisconsin. *Ecological monographs*, 27(4):326–349, 1957.
- Hugh A Chipman, Edward I George, and Robert E McCulloch. Bayesian cart model search. *Journal of the American Statistical Association*, 93(443):935–948, 1998.
- Hugh A Chipman, Edward I George, and Robert E McCulloch. Bart: Bayesian additive regression trees. *The Annals of Applied Statistics*, 4(1):266–298, 2010.
- Imre Csiszár. Eine informationstheoretische ungleichung und ihre anwendung auf beweis der ergodizitaet von markoffschen ketten. *Magyer Tud. Akad. Mat. Kutato Int. Koezl.*, 8:85–108, 1964.
- Mark Culp, Kjell Johnson, and George Michailidis. *ada: The R Package Ada for Stochastic Boosting*, 2016. URL <https://CRAN.R-project.org/package=ada>. R package version 2.0-5.
- Samuel Y Dennis III. On the hyper-dirichlet type 1 and hyper-liouville distributions. *Communications in Statistics-Theory and Methods*, 20(12):4069–4081, 1991.
- Marthinus Christoffel du Plessis, Hiroaki Shiino, and Masashi Sugiyama. Online direct density-ratio estimation applied to inlier-based outlier detection. *Neural Computation*, 27(9):1899–1914, 2015.
- Conor Durkan, Iain Murray, and George Papamakarios. On contrastive learning for likelihood-free inference. In *International conference on machine learning*, pages 2771–2781. PMLR, 2020.
- Jerome Friedman, Trevor Hastie, Robert Tibshirani, et al. Additive logistic regression: a statistical view of boosting (with discussion and a rejoinder by the authors). *Annals of statistics*, 28(2):337–407, 2000.
- Jerome H Friedman. Greedy function approximation: a gradient boosting machine. *The Annals of Statistics*, pages 1189–1232, 2001.
- Ian Goodfellow, Jean Pouget-Abadie, Mehdi Mirza, Bing Xu, David Warde-Farley, Sherjil Ozair, Aaron Courville, and Yoshua Bengio. Generative adversarial nets. *Advances in neural information processing systems*, 27, 2014.

- Peter Grünwald and Thijs van Ommen. Inconsistency of bayesian inference for misspecified linear models, and a proposal for repairing it. *Bayesian Analysis*, 12(4):1069–1103, 2017.
- Trevor Hastie, Robert Tibshirani, and Jerome Friedman. *The elements of statistical learning: data mining, inference, and prediction*. Springer Science & Business Media, 2009.
- Shohei Hido, Yuta Tsuboi, Hisashi Kashima, Masashi Sugiyama, and Takafumi Kanamori. Statistical outlier detection using direct density ratio estimation. *Knowledge and information systems*, 26(2):309–336, 2011.
- Chris C Holmes and Stephen G Walker. Assigning a value to a power likelihood in a general bayesian model. *Biometrika*, 104(2):497–503, 2017.
- Ian Holmes, Keith Harris, and Christopher Quince. Dirichlet multinomial mixtures: generative models for microbial metagenomics. *PloS one*, 7(2):e30126, 2012.
- Tetsuya Kaji and Veronika Ročková. Metropolis–hastings via classification. *Journal of the American Statistical Association*, 118(544):2533–2547, 2023.
- Takafumi Kanamori, Shohei Hido, and Masashi Sugiyama. A least-squares approach to direct importance estimation. *The Journal of Machine Learning Research*, 10:1391–1445, 2009.
- Adam Kapelner and Justin Bleich. bartmachine: Machine learning with bayesian additive regression trees. *Journal of Statistical Software*, 70:1–40, 2016.
- Masahiro Kato and Takeshi Teshima. Non-negative bregman divergence minimization for deep direct density ratio estimation. In *International Conference on Machine Learning*, pages 5320–5333. PMLR, 2021.
- Yoshinobu Kawahara and Masashi Sugiyama. Change-point detection in time-series data by direct density-ratio estimation. In *Proceedings of the 2009 SIAM international conference on data mining*, pages 389–400. SIAM, 2009.
- Patricio S La Rosa, J Paul Brooks, Elena Deych, Edward L Boone, David J Edwards, Qin Wang, Erica Sodergren, George Weinstock, and William D Shannon. Hypothesis testing and power calculations for taxonomic-based human microbiome data. *PloS one*, 7(12):e52078, 2012.
- Yaron Lipman, Ricky TQ Chen, Heli Ben-Hamu, Maximilian Nickel, and Matt Le. Flow matching for generative modeling. *arXiv preprint arXiv:2210.02747*, 2022.
- Song Liu, Makoto Yamada, Nigel Collier, and Masashi Sugiyama. Change-point detection in time-series data by relative density-ratio estimation. *Neural Networks*, 43:72–83, 2013.

Jason Lloyd-Price, Cesar Arze, Ashwin N. Ananthakrishnan, Melanie Schirmer, Julian Avila-Pacheco, Tiffany W. Poon, Elizabeth Andrews, Nadim J. Ajami, Kevin S. Bonham, Colin J. Brislawn, David Casero, Holly Courtney, Antonio Gonzalez, Thomas G. Graeber, A. Brantley Hall, Kathleen Lake, Carol J. Landers, Himel Mallick, Damian R. Plichta, Mahadev Prasad, Gholamali Rahnavaard, Jenny Sauk, Dmitry Shungin, Yoshiki Vázquez-Baeza, Richard A. White, Jason Bishai, Kevin Bullock, Amy Deik, Courtney Dennis, Jess L. Kaplan, Hamed Khalili, Lauren J. McIver, Christopher J. Moran, Long Nguyen, Kerry A. Pierce, Randall Schwager, Alexandra Sirota-Madi, Betsy W. Stevens, William Tan, Johanna J. ten Hoeve, George Weingart, Robin G. Wilson, Vijay Yajnik, Jonathan Braun, Lee A. Denson, Janet K. Jansson, Rob Knight, Subra Kugathasan, Dermot P. B. McGovern, Joseph F. Petrosino, Thaddeus S. Stappenbeck, Harland S. Winter, Clary B. Clish, Eric A. Franzosa, Hera Vlamakis, Ramnik J. Xavier, Curtis Huttenhower, and IBDMDB Investigators. Multi-omics of the gut microbial ecosystem in inflammatory bowel diseases. *Nature*, 569(7758):655–662, 2019. doi: 10.1038/s41586-019-1237-9. URL <https://doi.org/10.1038/s41586-019-1237-9>.

Li Ma and Wing Hung Wong. Coupling optional pólya trees and the two sample problem. *Journal of the American Statistical Association*, 106(496):1553–1565, 2011.

Koji Makiyama. *densratio: Density Ratio Estimation*, 2019. URL <https://CRAN.R-project.org/package=densratio>. R package version 0.2.1.

Jialiang Mao and Li Ma. Dirichlet-tree multinomial mixtures for clustering microbiome compositions. *The annals of applied statistics*, 16(3):1476, 2022.

XuanLong Nguyen, Martin J Wainwright, and Michael I Jordan. Estimating divergence functionals and the likelihood ratio by convex risk minimization. *IEEE Transactions on Information Theory*, 56(11):5847–5861, 2010.

Edoardo Pasolli, Lucas Schiffer, Paolo Manghi, Audrey Renson, Valerie Obenchain, Duy Tin Truong, Francesco Beghini, Faizan Malik, Marcel Ramos, Jennifer B Dowd, et al. Accessible, curated metagenomic data through experimenthub. *Nature methods*, 14(11):1023–1024, 2017.

Yury Polyanskiy and Yihong Wu. *Information theory: From coding to learning*. Cambridge university press, 2025.

Sashank Reddi, Barnabas Poczos, and Alex Smola. Doubly robust covariate shift correction. In *Proceedings of the AAAI conference on artificial intelligence*, volume 29, 2015.

Alfréd Rényi. On measures of entropy and information. In *Proceedings of the fourth Berkeley symposium on mathematical statistics and probability, volume 1: contributions to the theory of statistics*, volume 4, pages 547–562. University of California Press, 1961.

- Tommaso Rigon, Amy H Herring, and David B Dunson. A generalized bayes framework for probabilistic clustering. *Biometrika*, 110(3):559–578, 2023.
- Ruichen Rong, Shuang Jiang, Lin Xu, Guanghua Xiao, Yang Xie, Dajiang J Liu, Qiwei Li, and Xiaowei Zhan. Mb-gan: microbiome simulation via generative adversarial network. *GigaScience*, 10(2):giab005, 2021.
- Kris Sankaran, Saritha Kodikara, Jingyi Jessica Li, and Kim-Anh Lê Cao. Semisynthetic simulation for microbiome data analysis. *Briefings in Bioinformatics*, 26(1):bbaf051, 2025.
- Hidetoshi Shimodaira. Improving predictive inference under covariate shift by weighting the log-likelihood function. *Journal of statistical planning and inference*, 90(2):227–244, 2000.
- Jacopo Soriano and Li Ma. Probabilistic multi-resolution scanning for two-sample differences. *Journal of the Royal Statistical Society: Series B (Statistical Methodology)*, 79(2):547–572, 2017.
- Rodney Sparapani, Charles Spanbauer, and Robert McCulloch. Nonparametric machine learning and efficient computation with bayesian additive regression trees: The bart r package. *Journal of Statistical Software*, 97:1–66, 2021.
- Petar Stojanov, Mingming Gong, Jaime Carbonell, and Kun Zhang. Low-dimensional density ratio estimation for covariate shift correction. In *The 22nd international conference on artificial intelligence and statistics*, pages 3449–3458. PMLR, 2019.
- Masashi Sugiyama, Matthias Krauledat, and Klaus-Robert Müller. Covariate shift adaptation by importance weighted cross validation. *Journal of Machine Learning Research*, 8(5), 2007a.
- Masashi Sugiyama, Shinichi Nakajima, Hisashi Kashima, Paul Buenau, and Motoaki Kawanabe. Direct importance estimation with model selection and its application to covariate shift adaptation. *Advances in neural information processing systems*, 20, 2007b.
- Masashi Sugiyama, Taiji Suzuki, Shinichi Nakajima, Hisashi Kashima, Paul Von Bünau, and Motoaki Kawanabe. Direct importance estimation for covariate shift adaptation. *Annals of the Institute of Statistical Mathematics*, 60:699–746, 2008.
- Masashi Sugiyama, Ichiro Takeuchi, Taiji Suzuki, Takafumi Kanamori, Hirotaka Hachiya, and Daisuke Okanohara. Least-squares conditional density estimation. *IEICE Transactions on Information and Systems*, 93(3):583–594, 2010.
- Masashi Sugiyama, Taiji Suzuki, and Takafumi Kanamori. *Density ratio estimation in machine learning*. Cambridge University Press, 2012.
- Taiji Suzuki, Masashi Sugiyama, Takafumi Kanamori, and Jun Sese. Mutual information estimation reveals global associations between stimuli and biological processes. *BMC bioinformatics*, 10:1–12, 2009a.

- Taiji Suzuki, Masashi Sugiyama, and Toshiyuki Tanaka. Mutual information approximation via maximum likelihood estimation of density ratio. In *2009 IEEE International Symposium on Information Theory*, pages 463–467. IEEE, 2009b.
- Nicholas Syring and Ryan Martin. Calibrating general posterior credible regions. *Biometrika*, 106(2): 479–486, 2019.
- Owen Thomas, Ritabrata Dutta, Jukka Corander, Samuel Kaski, and Michael U Gutmann. Likelihood-free inference by ratio estimation. *Bayesian Analysis*, 17(1):1–31, 2022.
- Alexander Tong, Kilian Fatras, Nikolay Malkin, Guillaume Hugué, Yanlei Zhang, Jarrid Rector-Brooks, Guy Wolf, and Yoshua Bengio. Improving and generalizing flow-based generative models with minibatch optimal transport. *arXiv preprint arXiv:2302.00482*, 2023.
- Masatoshi Uehara, Masahiro Kato, and Shota Yasui. Off-policy evaluation and learning for external validity under a covariate shift. *Advances in Neural Information Processing Systems*, 33:49–61, 2020.
- Tao Wang and Hongyu Zhao. A dirichlet-tree multinomial regression model for associating dietary nutrients with gut microorganisms. *Biometrics*, 73(3):792–801, 2017.
- GA Whitmore and M Yalovsky. A normalizing logarithmic transformation for inverse gaussian random variables. *Technometrics*, 20(2):207–208, 1978.
- Makoto Yamada, Taiji Suzuki, Takafumi Kanamori, Hirotaka Hachiya, and Masashi Sugiyama. Relative density-ratio estimation for robust distribution comparison. *Neural computation*, 25(5):1324–1370, 2013.

Supplementary Materials

A Proofs

A.1 Proof of Proposition 2.1

We first fix the finite tree partition T_k . After adding the piece-wise constant function f_k , the loss is given by

$$l(w) = \sum_{A \in T_k} \left[e^{-\beta_k(A)} \int w_{k-1}^{-1} p d\mu + e^{\beta_k(A)} \int w_{k-1} q d\mu \right]$$

By the relationship between the arithmetic mean and the geometric mean, each summand is bounded below by

$$2\sqrt{\int w_{k-1}^{-1} p d\mu \int w_{k-1} q d\mu},$$

and the equality is attained if

$$e^{-\beta_k(A)} \int w_{k-1}^{-1} p d\mu = e^{\beta_k(A)} \int w_{k-1} q d\mu,$$

and this condition yields the expression for the optimal $\beta_k(A)$. Furthermore, when the lower bound is attained for all $A \in T_k$, the loss can be expressed as

$$l(w) = 2\sqrt{\int w_{k-1}^{-1} p d\mu \int w_{k-1} q d\mu},$$

and minimizing it with respect to T_k is equivalent to maximizing the discrete Hellinger loss given in the claim. \square

Also, we can derive the following corollary, by setting T_k to the root tree.

Corollary A.1. *Let w be the current estimate of the balancing function and c be the constant defined as $c = \sqrt{\mathbb{E}_p[w^{-1}]/\mathbb{E}_q[w]}$ and thus satisfies*

$$\mathbb{E}_p[(cw)^{-1}] = \mathbb{E}_q[(cw)].$$

Then the balancing loss is improved as

$$l(w) \geq l(cw).$$

A.2 Derivation of the regularized prior for the node parameters

According to Whitmore and Yalovsky (1978), when $W \sim \text{InverseGauss}(1, \theta)$ and θ are large, the distribution of the following variable is approximated by the standard normal distribution:

$$\frac{1}{2\sqrt{\theta}} + \sqrt{\theta} \log W.$$

Hence, when $\gamma_k(A) = e^{\beta_k(A)}$ follows $\text{InverseGauss}(1, K\lambda_0)$, the leaf node parameter $\beta_k(A)$ approximately follows

$$N\left(-\frac{1}{2\sqrt{K\lambda_0}}, \frac{1}{K\lambda_0}\right).$$

This observation implies that, under the prior

$$\gamma_k(A) \sim \text{InverseGauss}(1, K\lambda_0) \ (k : \text{odd}), \ \gamma_k(A)^{-1} \sim \text{InverseGauss}(1, K\lambda_0) \ (k : \text{even}),$$

the distribution of $\log w$ is approximated by $N(0, \lambda_0^{-1})$.

B Details of the posterior sampling for the Bayesian additive tree model

B.1 MCMC algorithm

The Bayesian additive model includes three types of unknown variables: (i) tree partition structures T_1, \dots, T_K , (ii) leaf node parameters β_1, \dots, β_K , where β_k denotes the collection of the parameters for the k th basis function, and (iii) the temperature τ . Their posterior distributions are estimated with the following Metropolis-within-Gibbs algorithm:

1. For $k = 1, \dots, K$,
 - (a) Compute the residual $\log w_{-k} = \sum_{l \neq k} f_l$.
 - (b) Update $T_k \mid w_{-k}, \tau$.
 - (c) Update $\beta_k \mid w_{-k}, T_k, \tau$.
2. Update $\tau \mid w$, where w is the current balancing weight.

Updating the node parameters β_k and the temperature τ is straightforward due to their conjugate structures. The algorithm to update T_k with the Metropolis-Hastings algorithm is detailed in the next section.

B.2 Updating trees

In this section, we consider updating the k th tree denoted by T_k given the other parameter values using the proposals originally introduced for the Bayesian CART model (Chipman et al., 1998), and the details are obtained by following Kapelner and Bleich (2016).

In each iteration of the MCMC, we propose a new tree structure T_K^* by modifying the current tree T_k via one of the three moves, GROW, PRUNE, and CHANGE, defined as follows:

GROW: Randomly select one leaf node and split it to generate two child nodes.

PRUNE: Randomly select one second-generation internal node (2GI), that is, a node with two child nodes that are terminal, and remove these child nodes.

CHANGE: Randomly select one 2GI node and change the splitting rules by sampling a new rule from the prior distribution.

One of the moves is selected stochastically according to the fixed probabilities $p(\text{GROW})$, $p(\text{PRUNE})$, and $p(\text{CHANGE})$, and they are set to $1/3$ in our numerical experiments.

Let T_k^* denote the new proposed tree structure. Then, the proposal is accepted with probability $\min\{\alpha, 1\}$, where

$$\alpha = \frac{\underbrace{p(T_k^*)}_{\text{Prior}} \underbrace{p(T_k^* \rightarrow T_k)}_{\text{Transition}} \underbrace{p(\text{data} \mid T_k, p(\{w_{-k}(x_i)\}_{i=1}^n))}_{\text{Loss-based likelihood}}}{\underbrace{p(T_k)}_{\text{Prior}} \underbrace{p(T_k \rightarrow T_k^*)}_{\text{Transition}} \underbrace{p(\text{data} \mid T_k^*, p(\{w_{-k}(x_i)\}_{i=1}^n))}_{\text{Loss-based likelihood}}}$$

and $\{w_{-k}(x_i)\}_{i=1}^n$ are the residuals. If a node A is selected for updating T_k , then the ratios corresponding to the priors and the transition probabilities for the three moves are given as

$$\frac{p(T_k^*) p(T_k^* \rightarrow T_k)}{p(T_k) p(T_k \rightarrow T_k^*)} = \begin{cases} \frac{a_T(1-a_T(2+\text{depth}(A))^{-b_T})^2}{(1+\text{depth}(A))^{b_T}-a_T} \frac{\# \text{ leaf nodes in } T_K}{\# \text{ 2GI nodes in } T_K^*} & (\text{GROW}), \\ \frac{(1+\text{depth}(A))^{b_T}-a_T}{a_T(1-a_T(2+\text{depth}(A))^{-b_T})^2} \frac{\# \text{ 2GI nodes in } T_K}{\# \text{ leaf nodes in } T_K^*} & (\text{PRUNE}) \\ 1 & (\text{CHANGE}). \end{cases}$$

(see Kapelner and Bleich (2016) for further details.)

For calculating the likelihood ratios, we need to note that we can analytically evaluate the likelihood with the leaf node parameters integrated out due to conjugacy as follows:

$$\int p(\beta_k) L_{n,\tau}(w) d\beta_k \propto \prod_{A \in \mathcal{L}(T_k)} L_{k,A},$$

where $p(\beta_k)$ is the joint prior density of the leaf node parameters, $\mathcal{L}(T_k)$ is the collection of the leaf nodes, and

$$L_A = \sqrt{\frac{\lambda_k(A)}{\lambda'_k(A)}} \exp\left(\frac{\lambda_k(A)}{\mu_k(A)} - \frac{\lambda'_k(A)}{\mu'_k(A)}\right).$$

Hence, for the GROW move in which the node A is split into A_l and A_r , the likelihood ratio is given as

$$\frac{L_{A_l} L_{A_r}}{L_A},$$

while in the PRUNE move, which removes A_l and A_r , the ratio is the inverse. The CHANGE move generates two new children A_l^* and A_r^* , so the likelihood ratio is given as

$$\frac{L_{A_l^*} L_{A_r^*}}{L_{A_l} L_{A_r}}.$$

C Details of experiments

C.1 2-dimensional numerical experiments

The parameters for simulating the data sets are specified as follows:

2. Local shift $\mu_1 = (9.0, 9.9)'$, $\mu_2 = (-2.5, 1.4)'$, $\mu_3 = (-2.3, -9.7)'$, $\mu_4 = (3.4, 5.9)'$, $\mu_5 = (5.8, -9.5)'$,
 $(\Sigma_1(1, 1), \Sigma_1(1, 2), \Sigma_1(2, 2)) = (2.9, 0.5, 1.1)$, $(\Sigma_2(1, 1), \Sigma_2(1, 2), \Sigma_2(2, 2)) = (1.2, -0.6, 2.8)$,
 $(\Sigma_3(1, 1), \Sigma_3(1, 2), \Sigma_3(2, 2)) = (2.3, -1.0, 1.7)$, $(\Sigma_4(1, 1), \Sigma_4(1, 2), \Sigma_4(2, 2)) = (1.1, -0.4, 2.9)$,
and $(\Sigma_5(1, 1), \Sigma_5(1, 2), \Sigma_5(2, 2)) = (3.0, 0.2, 1.0)$.

3. Local dispersion difference $\mu_1 = (1.9, -7.2)'$, $\mu_2 = (-5.7, 5.3)'$, $\mu_3 = (-2.3, -1.5)'$, $\mu_4 = (7.5, -3.1)'$, $\mu_5 = (3.1, 9.5)'$, $(\Sigma_1(1, 1), \Sigma_1(1, 2), \Sigma_1(2, 2)) = (1.0, -0.4, 0.8)$,
 $(\Sigma_2(1, 1), \Sigma_2(1, 2), \Sigma_2(2, 2)) = (1.3, 0.7, 2.7)$, $(\Sigma_3(1, 1), \Sigma_3(1, 2), \Sigma_3(2, 2)) = (1.0, 0, 3.0)$,
 $(\Sigma_4(1, 1), \Sigma_4(1, 2), \Sigma_4(2, 2)) = (2.9, 0, 1.1)$, and $(\Sigma_5(1, 1), \Sigma_5(1, 2), \Sigma_5(2, 2)) = (2.4, -0.9, 1.6)$.

C.2 20-dimensional dimensional experiments

μ_1 is set to $(-0.5, 0, 0, 0)'$ in the location shift scenario and $(0, 0, 0, 0)'$ in the dispersion difference scenario. The other parameters are fixed as $\mu_2 = (0, 0, 0, 0)'$, $\Sigma_1 = I_4$, and $\Sigma_2 = 4I_4$ in both scenarios.

C.3 Notes on the implementation of the density ratio estimators

In the proposed boosting algorithms, we prune leaf nodes that contain observations from only one group to avoid division by zero in computing the optimal values of leaf node parameters.

For AdaBoost, we used the `ada` function from the `ada` package (Culp et al., 2016), and the optimal number of trees is selected via the 5-fold cross-validation based on the classification error reported by the function. We found that the selected number tends to be close to zero when the two-sample difference is small (such as the local shift scenario in the 2D experiments), so we set the minimum number of trees to 10 manually.

For the KLIEP and uLSIF, we use the functions `KLIEP` and `uLSIF` from the R package `densratio` (Makiyama, 2019) with the default parameter values. It should be noted that we detected an error in the source code for the `KLIEP` function ¹, so we used a fixed version that is available at <https://github.com/nawaya040/densratio>.

¹The estimated density ratios are not correctly computed on observations in a test data set in the original package.

D Additional figures

We provide additional visualizations corresponding to the settings described in Section 4.1. Figure 8 shows the estimated log-density ratios for the first (global shift) and third (local dispersion difference) scenarios under the balanced sample size setting, and Figure 9 shows the estimated ratios for the second (local shift) scenario under the unbalanced sample size configuration.

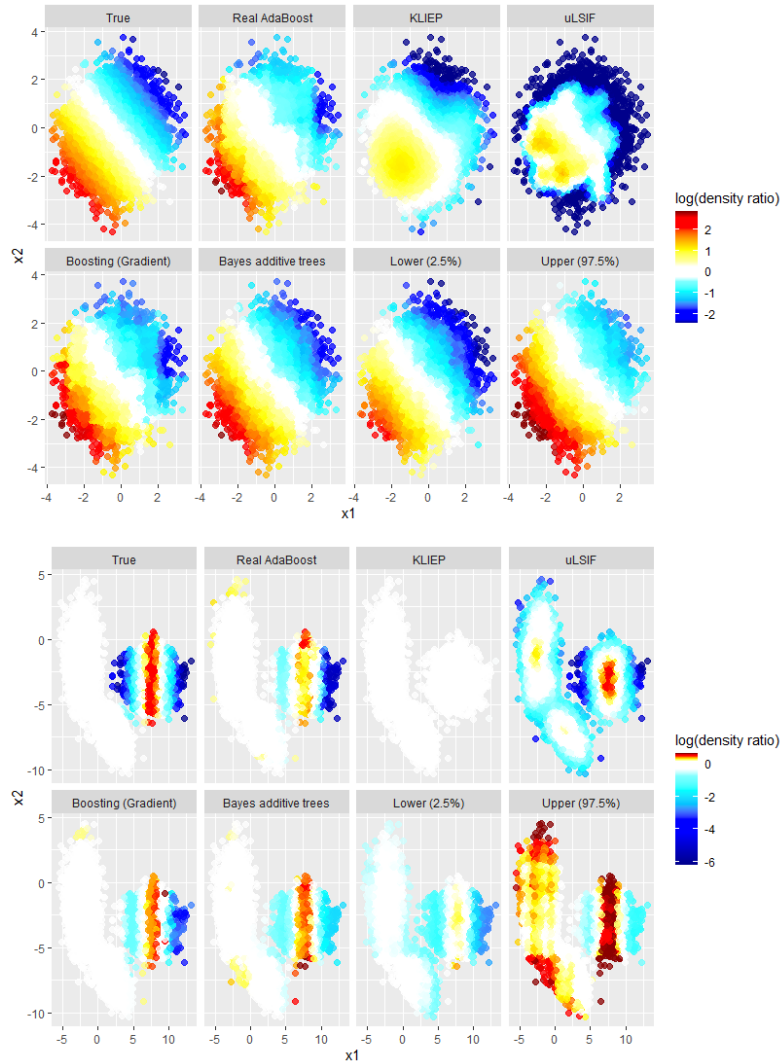


Figure 8: The estimated log-density ratios obtained using the algorithms considered in the two-dimensional examples for the global shift scenario and the local dispersion scenario ($n_0 = n_1 = 5000$). For the Bayesian additive model, the 2.5% quantiles and 97.5% quantiles of the log-density ratios evaluated point-wise are also displayed. The difference between FS and GB is minimal, so we present only the results for GB.

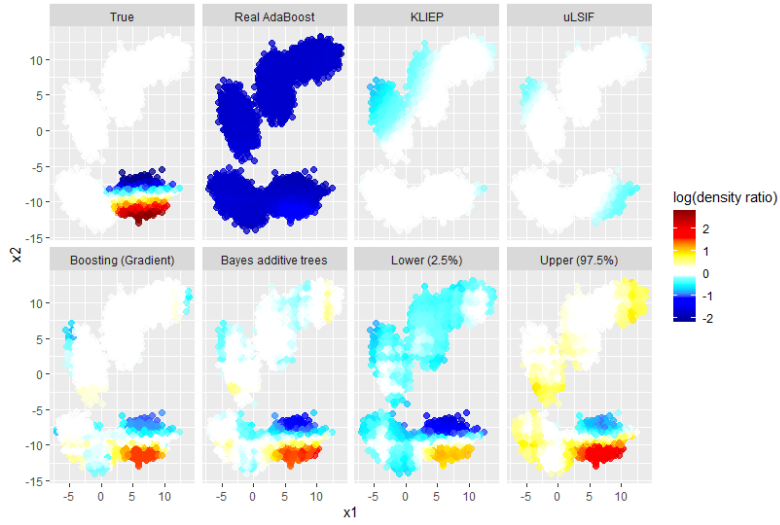


Figure 9: The estimated log-density ratios obtained with the algorithms considered in the two-dimensional examples for the global shift scenario and the local dispersion scenario ($n_0 = 9000$ and $n_1 = 1000$). For the Bayesian additive model, the 2.5% quantiles and 97.5% quantiles of the log-density ratios evaluated point-wise are also displayed. The difference between FS and GB is minimal, so we present only the results for GB.